The Impact of Hazardous Terrain on Lunar Landing Performance

Christopher Glaser[1,2], Taro Kawano[2,3], Yusuke Maru[2] and Shujiro Sawai[2]

***Abstract*—On September 13, 1959 the spacecraft *Luna 2* of the Soviet Union was the first man made object to successfully reach the lunar surface. Since then, there have been 20 successful soft Moon landings, both manned and unmanned, preferably on relatively smooth and level terrain. Current Moon missions are being targeted more and more at hazardous landing sites like craters, the far side of the Moon and in polar regions. This trend increases requirements and demands on robust landing methods and lander designs. The authors investigate the effect of terrain roughness, slope and uncertain initial landing conditions using a randomized boulder size-frequency distribution and terrain slope algorithm. Starting point of the lander design is the *Surveyor* program of NASA (1966-1968). The multibody dynamics simulation software Adams is used to carry out an extensive parameter and sensitivity study using the Monte Carlo approach to evaluate landing success rates.**

***Index Terms*—Landing Dynamics, Hazardous Terrain Generation, Surveyor, Adams**

I. Introduction

THE scope of this paper is to derive recommendations for lander designs that are targeted at hazardous terrains. Starting with *Chang'e 4*, the international space community began targeting future missions at rough terrain and polar regions. This is driven by the fact that the far side of the Moon and polar regions have considerably higher scientific importance compared to the near side of the Moon and improving technology allows for more sophisticated missions. Landing near or inside craters – and therefore hazardous terrain – has two main scientific advantages:

- Next to craters, a lot of ejecta from impacts of asteroids and comets can be easily collected without needing to drill. The Atkin Basin at the South Pole is the largest known impact crater in the solar system. Examining these areas of impact can lead to understanding the creation of the Earth-Moon system.[1]
- Craters in the South Pole region of the Moon have shown evidence of frozen water. Investigating and/or sampling ice on the Moon will greatly improve mankinds understanding of the creation of life and the universe.[2]

All things considered, the motivation to research landing performance on hazardous terrain is considerably high. To investigate the impact of this terrain, the authors carried out three steps: First, a randomized terrain algorithm was developed to be able to generate hazardous terrain effectively. Second, the lander design of the NASA's *Surveyor* program was implemented into the Adams environment. Since NASA published a majority of the scientific data of the *Surveyor* program, it is an ideal starting point in investigating landing performance.[3] In a last step, an extensive Monte Carlo study was carried out to derive the effect hazardous terrain has on both the landing performance and the lander design.

Manuscript received August 30, 2019
[1]RWTH Aachen University
[2]Institute of Space and Astronautical Science, JAXA
[3]Research and Development Directorate, JAXA

II. Randomized Terrain Algorithm

The design process of the randomized terrain algorithm is divided into two parts, which are reflected in the following two sections: At the beginning, it is decided which tasks and functions the algorithm has to cover to be able to generate random terrains and a mathematical model is developed to implement the desired mode of operation into a programming code to enable the user to automate the randomized terrain generation process (see Section II-A). Finally, the algorithm is validated in Section II-B.

A. Development

Hazardous terrain can be described as number and size of rocks and the slope of the mean plane. Slope is defined as the deviation of the plane relative to a local horizon (see Figure 1). In this paper it is expressed in degrees. Roughness, on the other hand, is the variation from the mean plane.[4] Within the scope of this research, roughness is referred to as number and height of boulders. The dimensions of a boulder are set by the parameters height (H) and diameter (D). Observations of lunar landing sites revealed a correlation between height and diameter, which can be expressed as $\frac{H}{D} \sim 0.54 \pm 0.03$.[5] Therefore, the recommendation of Demidov and Basilevsky to apply a value of 0.5 for engineering applications is followed.[5]

The distribution of boulders follows the so-called Rock Size-Frequency Distribution (RSFD). This model assigns each

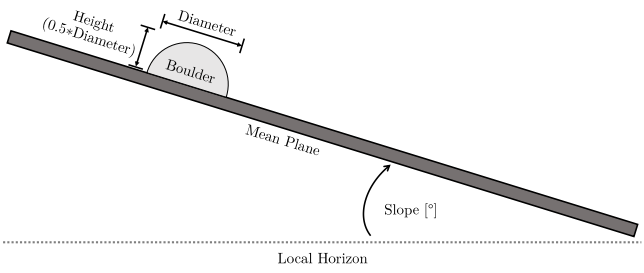

Fig. 1. Definition of terrain characteristics

rock size a number of occurrences. Using RFSD, each landing site can be described and characterized by an individual Rock Size-Frequency Distribution. If needed, a power law curve fit can be added to develop a mathematical model. In general, it is defined as [6]

$$N_{\text{boulder}}(D_i) = k \cdot e^{-l \cdot D_i} \ . \tag{1}$$

where $N_{\text{boulder}}(D_i)$ is the absolute number of boulders per diameter and k and l are site specific parameters. Varying these parameters, different sites can be modeled. From here on, the k and l parameters are set to 193.2 and 16.77 respectively. Although these parameter values represent in fact the RFSD at the *Change'e 3* landing site as observed by Di et al.[6], they also quantify the average of the different site parameters of the *Surveyor* landing sites.[6]

Having defined hazardous terrain, the mode of operation of the randomized terrain algorithm can be summarized as follows:

> Randomized generation of *n* boulders following a modifiable rock size-frequency distribution on a predefined but adjustable area.

To achieve this, the algorithm has to fulfill three tasks:

1) Distribution of *n* boulders on a predefined area using pseudo-randomly generated x- and y-coordinates for each rock. At this stage, the boulders have no geometric properties.
2) Calculation of the likelihood that a boulder has a certain diameter and height according to the RSFD parameters k and l.
3) Assignment of a diameter for each boulder based on the probability calculated in the second step.

The first step is achieved by the *rand()* function of MATLAB, which calculates uniformly distributed values between 0 and 1. It is used to randomly generate x- and y-coordinates for each boulder within the width and length boundaries of a predefined area. The upper and lower boundary of the terrain dimensions are labeled $x_{\text{max}}/x_{\text{min}}$ and $y_{\text{max}}/y_{\text{min}}$ respectively; the position is well-defined by the x- and y-coordinates:

$$\begin{aligned} x_i &= x_{\text{min}} + (x_{\text{max}} - x_{\text{min}}) \cdot \text{rand()} \\ y_i &= y_{\text{min}} + (y_{\text{max}} - y_{\text{min}}) \cdot \text{rand()} \\ (x_i, y_i) &= pos_{\text{boulder},i} \end{aligned} \tag{2}$$

Equation (2) is repeated for all *n* boulders. The result is a terrain with pseudo-randomly distributed boulders without geometric properties.

For the second step, the likelihood of each boulder having a certain diameter is calculated. Therefore, the total number of rocks having a diameter between 0.1 and 0.5 m is determined in Equation (3). These limits are chosen because rocks below a diameter of 0.1 m are not considered critical for landing performance, and diameters above 0.5 m can be detected and actively avoided in the final descent phase.[7] The total number of rocks in the range of $D = 0.1 - 0.5$ m gives:

$$N_{\text{total}} = \sum_{j=10}^{n=50} k \cdot e^{-l \cdot \frac{j}{100}} \ . \tag{3}$$

Using (3), the likelihood of a boulder having a certain diameter can be calculated as

$$\text{prob}(D_i) = \frac{N_{\text{boulder}}(D_i)}{N_{\text{total}}} = \frac{k \cdot e^{-l \cdot D_i}}{\sum_{j=10}^{n=50} k \cdot e^{-l \cdot \frac{j}{100}}} \ . \tag{4}$$

Equation (4) allows for an efficient calculation of each probability. In a final step, the calculated likelihoods are assigned to the x- and y-coordinates generated in (2). The height of a boulder is set to half the diameter value following the recommendation of Demidov and Basilevsky.[5] Finally, the algorithm is executed and the terrain model generated is transferred into the Adams environment. The procedure described above is now defined as a function called *random_boulders()* in the MATLAB environment for convenient access. The syntax for execution is as follows:

$$\text{random\_boulders}\ (n,\ x_{\text{min}},\ x_{\text{max}},\ y_{\text{min}},\ y_{\text{max}},\ k,\ l) \tag{5}$$

n : Number of boulders
x_{min}/x_{max} : Terrain boundaries (width)
y_{min}/y_{max} : Terrain boundaries (depth)
k/l : Site specific RFSD parameter

The results of the terrain algorithm implemented in Adams on a terrain of 100 m^2 with a boulder range from 40 to 200 are depicted in Figure 2.

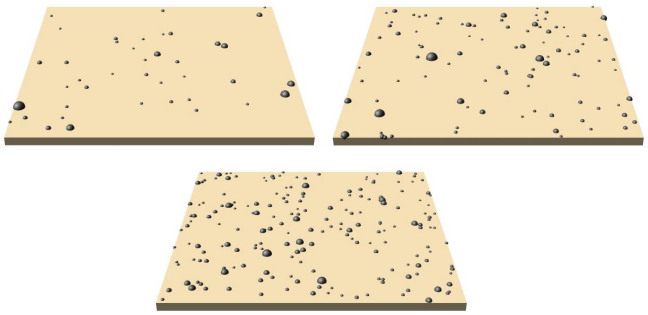

Fig. 2. Terrain algorithm for 40, 100 and 200 boulders

B. Validation

In Figure 2, it could be observed that the randomized terrain algorithm generates qualitatively correct results. To validate the algorithm quantitatively, the approach is the following: Let the algorithm generate four different randomized terrains with the number of boulders being 100, 500, 1000 and 2000 on 100 m^2. After the boulders are generated, the terrain is split up into four smaller areas and the rocks are counted separately in each quarter. Further, the number of rocks are plotted against the RFSD that they are supposed to match. The described approach enables a validation of the randomized terrain algorithm in two ways:

1) It can be investigated whether the diameter allocation follows the implemented RFSD.
2) Because the terrain is split up into quarters, it can be validated if the positions of the boulders are distributed randomly and the algorithm therefore is valid both on the whole terrain and in each quarter independently.

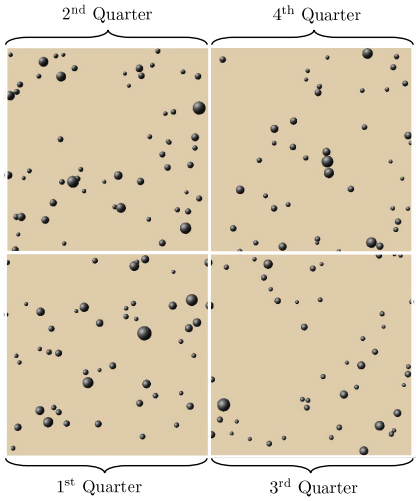

Fig. 3. Top view of the generated terrain and its division into four quarters

The approach is visualized in Figure 3. The validation results are summarized in Figures 4 and 5. The abscissa displays the diameter while the rock count in each quarter is documented in the ordinate. Colored bars for each quarter represent the number of rocks counted. Within the Figures the total number of rocks is increased from 100 to 2000. The red line in each diagram represents the RFSD proposed by Di et al.[6] that is implemented in the terrain algorithm. The closer the bars match the red line – and therefore the implemented RFSD – the more accurate the algorithm distributes the the boulders according to the mathematical model underneath.

In Figure 4, it can be found that the distribution of boulder diameters follows the implemented RFSD, but since the sample size is rather small, some statistical perturbations remain. In Figure 5, the deviations from the RFSD become negligible. This proves that the developed terrain algorithm is working as desired and the perturbation in smaller sample sizes like in Figure 4 are due to stochastic reasons and not caused by a fault in the algorithm. The algorithm can therefore be assumed fully validated.

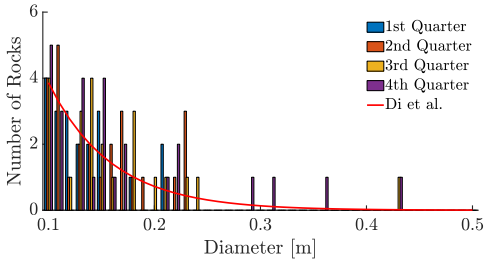

Fig. 4. Total number of boulders: 100

III. Development and Validation of Surveyor Model

To be able to implement the *Surveyor* geometry into Adams, the relevant real world characteristics of the landing gear need to be identified and quantified. Furthermore, the *Surveyor* data need to be idealized and translated into a multibody

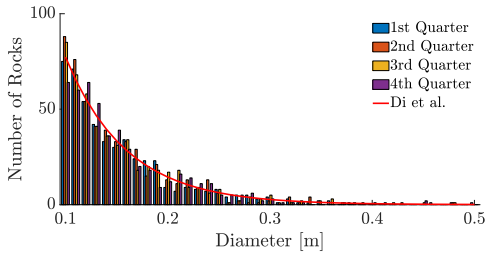

Fig. 5. Total number of boulders: 2000

dynamics model. This is carried out in Section III-A. After the idealization is implemented in the Adams environment, the model is validated by reenacting three *Surveyor* landings and comparing the landing dynamics of historical data from the Moon and the Adams generated data.

A. Idealization

Surveyor is a three-legged lander with an aluminum spaceframe as main body. Each leg consists of one primary and two secondary aluminum struts hinged to the main frame. A crushable aluminum honeycomb foot pad is attached to the struts by using a hinge. Three aluminum honeycomb body blocks are positioned below the main body.[3] The primary strut is equipped with a shock absorber consisting of a hydraulic cylinder and a piston. The arrangement of the primary and secondary struts is called inverted tripod type.[8] The Purpose of the shock absorber and honeycomb blocks is the dissipation of the kinetic energy of the lunar landing.[3] Figure 6 depicts the exact dimensions of the *Surveyor* landing gear.

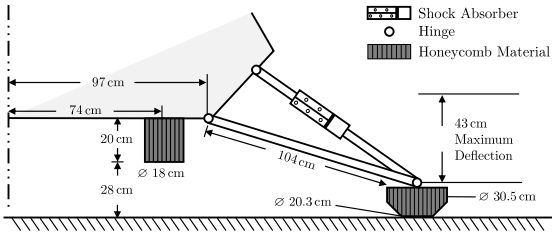

Fig. 6. Schematic drawing of *Surveyor* landing gear (based on [3])

The idealization of the *Surveyor* geometry utilizes the following elements:

- **Bodies** rigid or flexible, inheriting geometry and mass properties.
- **Connectors** like springs and damper elements, connecting the bodies.
- **Constraints** like forces and hinges, enabling or restricting movement.

Summarizing the *Surveyor* idealization, it is a rigid main body with spring-damper systems as struts. The honeycomb crush elements are modeled as forces and the contact between lander geometry and terrain is approximated by a spring damper system with a Coulomb friction force model. The main body is chosen to be rigid, since the eigenfrequency and oscillations of the flexible real world *Surveyor* structure

were observed to only contribute 1 mm of vibration movement to the spacecraft's total motion.[3] Defining the main body as rigid in the simulations greatly improves simulation efficiency while still maintaining accurate results. The mean lunar gravity is approximately one sixth of Earth's gravity, hence $g_{\text{lunar}} \approx 1.624\,\text{m/s}^2$.[9] Figure 7 summarizes the idealization in a schematic drawing, whereas Figure 8 displays the final geometry in the Adams environment.

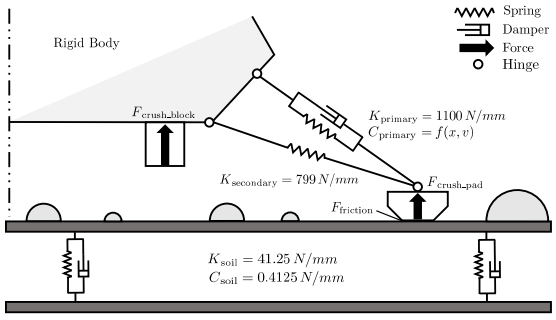

Fig. 7. Idealized *Surveyor* landing gear

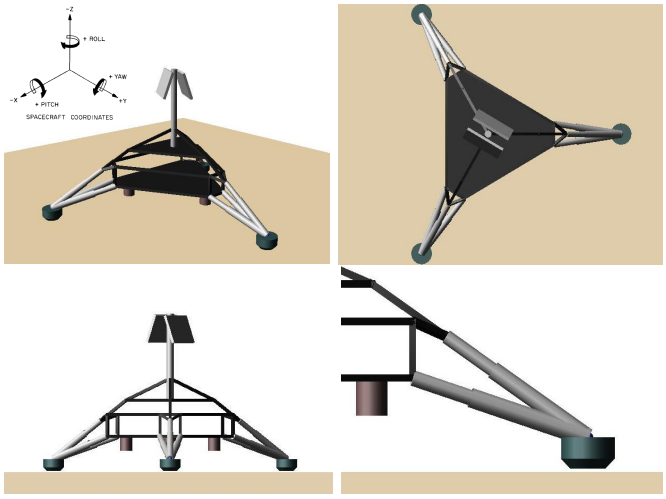

Fig. 8. *Surveyor* Adams model

B. Validation

The approach to validate the Adams model is straight forward. NASA published the majority of the *Surveyor* program data. This data include information on the spacecraft as well as landing dynamics and details of observed landing dynamics.[3] This allows for checking the Adams model against real world landing data. Of special interest for validation are the force readings of the shock absorber of the primary strut in each of the three legs. During the landings, the *Surveyor* spacecraft sent an analogous signal of the force readings to Earth via telemetry.[3] Therefore, the validation approach is to reenact two *Surveyor* landings in the Adams environment knowing the initial conditions of each landing. Comparing the shock absorber readings enables to validate the Adams model in two ways:

- It can be validated whether the peak values and the subsequent oscillations of the Adams and NASA datasets are in the same order of magnitude. Checking this, it can be derived whether the energy is absorbed sufficiently.
- The period between force peaks (maximum deflection) and zero force readings (rebound) gives a quick confirmation on whether the *Surveyor* and its Adams model perform the same way during the touchdown phase.

Figures 9 and 10 document the validation results. The gray line represents the NASA data collected from the *Surveyor* landings, and the Adams simulated force readings are displayed as the red dotted line. It can be observed that the overall fit of the Adams force readings regarding the NASA data is very good. In detail, the value of the initial peak is similar in all cases and the slope of the force readings are nearly the same. This indicates that the contraction at contact is modeled almost perfectly. Therefore, the shock absorbing behavior is in good agreement. Also, the zero force readings and their period are in good correlation with the NASA data. Nevertheless, the NASA data include oscillations even during the zero force readings. The Adams data do not contain these oscillations. This effect is explained as follows: The Adams main body was modeled as rigid body. Therefore, it can neither vibrate nor deform. In other words, the stiffness and damping of the main body is infinite – no oscillations are possible. That is why the red dotted line is flat. Summarizing Figures 9 and 10, the *Surveyor* Adams model can be considered validated.

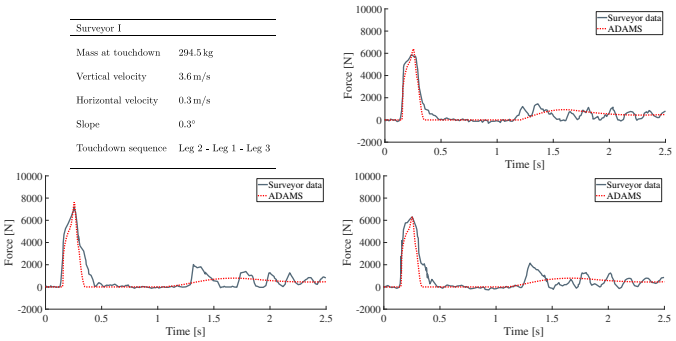

Fig. 9. Validation of *Surveyor I* landing for all three legs

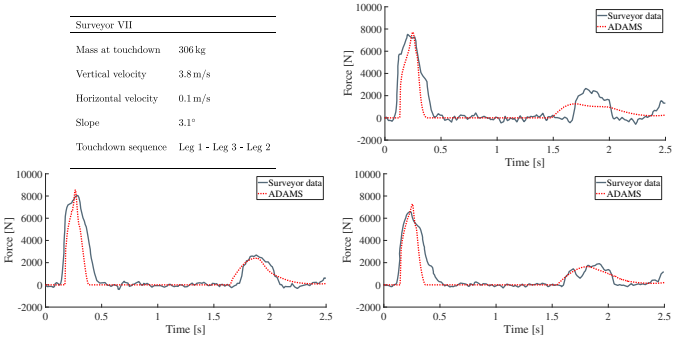

Fig. 10. Validation of *Surveyor VII* landing for all three legs

IV. Assessment of Landing Performance

In the next two Sections, the terrain algorithm and the *Surveyor* Adams model will be combined to judge success rates on different terrains. The simulation setup will be explained in Section IV-A and the simulations are carried out in Section IV-B.

A. Simulation Approach

To judge landing performance of the *Surveyor* the approach is the following:

1) Create 12 different terrains with different roughness (number of rocks) and slope parameters.
2) Distribute the initial landing conditions of *Surveyor* model in a Monte Carlo approach to simulate the uncertainty of initial conditions.
3) Judge the success rate on each of the 12 terrains.

Table I lists the distribution of initial conditions prior to touchdown. The boundaries are set according to NASA recommendations in the *Surveyor* era.[10] The 12 different terrains that are generated and their respective Case ids are displayed in Table II. Basically, the slope is increased from 0° to 20°. This corresponds to the minimum and maximum slope encountered during the *Surveyor* program. The number of rocks is chosen to represent the total number of rocks on 100 m^2 area for the landings of *Surveyor I* ($\approx$ 40), *Apollo 16* ($\approx$ 100) and *Surveyor II* ($\approx$ 200).[6] Three terrains without rocks are implemented for better comparison. Landing success is based on three criteria:

1) Did the lander tumble?
2) Was a rock contacted?
3) Was the contact critical? (>5000 N)

A total of 2400 simulations will be conducted to create a large enough sample size.

TABLE I
Distribution of Initial Conditions

Parameter	Initial pitch	Initial roll	Initial yaw
Distribution Boundaries	Gaussian $\mu = 0°$ $3\sigma = 5°$	Uniform $0 - 360°$	Gaussian $\mu = 0°$ $3\sigma = 5°$

Parameter	Vertical velocity	Horizontal velocity
Distribution Boundaries	Gaussian $\mu = 3.9$ m/s $3\sigma = 0.3$ m/s	Gaussian $\mu = 0$ m/s $3\sigma = 0.3$ m/s

B. Results

The success rates for each landing are displayed in Figure 11. It is evident, that the success rates on terrain without boulders are almost 100%. This is in good agreement with the real landing of *Surveyor V* that landed safely up until 20° slope. It can be clearly observed that the risk of a rock contact increases with the roughness of the terrain. Also, once roughness is introduced to a terrain, the cases of tumbling increase. Nevertheless, tumbling is not the critical part in the success rates of the *Surveyor* model. The mission is way more likely to be not successful due to rock contacts. This is explained in revisiting Figure 6: The *Surveyor* model has a very small ground clearance of 200 mm once the curshblocks contact the surface. This means every rock bigger than 200 mm will contact the structure and render the mission unsuccessful. It seems that NASA chose landing stability over rock contacts. The center of gravity is very low, which allows for really stable landings and trading of ground clearance. Another effect worth mentioning is that the number of rock contacts decreases with increasing slope. This effect is explained as follows: On flat surface, all three legs will contact the surface almost simultaneously. Therefore the deflection of the *Surveyor* model is considerably high and the main body will approach the surface horizontally, which leads to a big area of attack. On the other hand, if the lander lands on a slope, first one or two legs will contact and absorb a large amount of energy while the main body is tilted towards the ground. This increases the chances of the lander to evade rock contact.

TABLE II
Definition of Case id's

Case id	S0N0	S0N40	S0N100	S0Nb200
Slope	0°	0°	0°	0°
Number of rocks	0	40	100	200
Case id	S10N0	S10N40	S10N100	S10N200
Slope	10°	10°	10°	10°
Number of rocks	0	40	100	200
Case id	S20N0	S20N40	S20N100	S20N200
Slope	20°	20°	20°	20°
Number of rocks	0	40	100	200

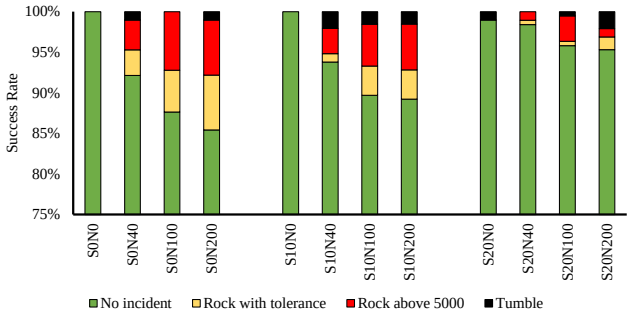

Fig. 11. Success rate for *Surveyor* model

To prove, that NASA in fact chose stable landing over ground clearance, the design of the *Surveyor* model was adjusted to allow for more ground clearance. The ground clearance was doubled to 400 mm. Figure 12 shows both the initial design and the design with the increased ground clearance. The leg lengths were kept the same and only the leg angle was adjusted to assure the adjusted model does not disagree with the limitations of the launch vehicle. After the *Surveyor* model was adjusted, an additional 2400 studies were conducted to judge the success rates of the new model. The simulation set up is identical to Table I and II. The results are documented in Figure 13. It can be seen that the hypothesis of the trade off between ground clearance and stability was

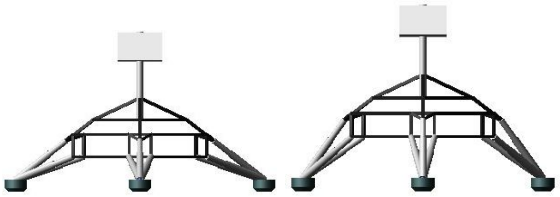

Fig. 12. Initial design (left) and increased ground clearance (right)

right. It becomes evident, that the model with the increased ground clearance shows no rock contacts whatsoever. The success rate on flat terrains is superior to the initial model. It is in the higher slope areas with high roughness, where it becomes clear that the new model is very unstable on rougher terrain. While the initial model showed very little tumbling even on very hazardous terrain, the new model becomes very unstable on steep terrain. In a further study, the critical slope for both designs was evaluated to quantify the difference in stability on slope. The initial design was stable up to 40° slope, whereas the model with the increased ground clearance was already unstable at 28° slope. This means NASA tried to design *Surveyor* as a very stable lander, with taking the risk of a rock contact. A choice that is reasonable considering it was NASA's first attempt at soft lunar landings.

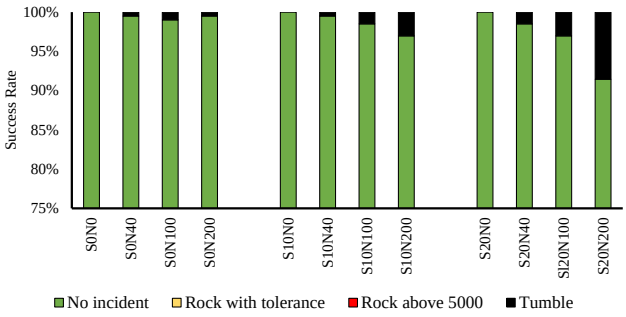

Fig. 13. Success rate for model with increased ground clearance

V. Conclusion

In summary, this paper addresses the impact of hazardous terrain on the performance and the design of a lander. First, a terrain algorithm was developed to randomize hazardous terrain generation. Afterwards, the lander design of the *Surveyor* program was implemented into Adams. In a Monte Carlo analysis, the success rates of the *Surveyor* model were judged. It became clear, that the main threat for the *Surveyor* model were rock contacts rather than tumbling. To investigate the cause of this effect, the *Surveyor* design was adjusted to increase ground clearance. This step allowed to demonstrate, how a higher ground clearance diminishes rock contacts while drastically increasing stability. Increasing the ground clearance 200 mm already decreased the maximum theoretically allowed slope from 40° to 28°. Summarizing this paper, it can be said that hazardous terrain calls for a decision: Either decrease ground clearance to increase stability and the risk of contacting boulders, or increase ground clearance to avoid rocks while drastically decreasing stability.

References

[1] D. Koebel, M. Bonerba, D. Behrenwaldt, M. Wieser, and C. Borowy, "Analysis of landing site attributes for future missions targeting the rim of the lunar South Pole Aitken basin," *Acta Astronautica*, vol. 80, pp. 197–215.

[2] M. Litvak, "The vision of the Russian Space Agency on the Robotic Settlements in the Moon."

[3] E. M. Shoemaker, E. C. Morris, R. M. Batson, H. E. Holt, K. B. Larson, Montgomery, J. J. Rennilson, and E. A. Whitaker, "Surveyor: Program Results," *NASA SP-184*.

[4] M. A. Rosenburg, O. Aharonson, J. W. Head, M. A. Kreslavsky, E. Mazarico, G. A. Neumann, D. E. Smith, M. H. Torrence, and M. T. Zuber, "Global surface slopes and roughness of the Moon from the Lunar Orbiter Laser Altimeter," *Journal of Geophysical Research*, vol. 116, no. E2, p. E11007.

[5] N. E. Demidov and A. T. Basilevsky, "Height-to-diameter ratios of moon rocks from analysis of Lunokhod-1 and -2 and Apollo 11–17 panoramas and LROC NAC images," *Solar System Research*, vol. 48, no. 5, pp. 324–329.

[6] K. Di, B. Xu, M. Peng, Z. Yue, Z. Liu, W. Wan, L. Li, and J. Zhou, "Rock size-frequency distribution analysis at the Chang'E-3 landing site," *Planetary and Space Science*, vol. 120, pp. 103–112.

[7] K. Matsumoto, S. Sasa, Y. Katayama, and T. Sugihara, "Probabilistic obstacle avoidance strategy for safe and soft moon landing," in *ISAS proceedings of 14th Workshop on Astrodynamics and Flight Mechanics 2004: A Collection of Technical Papers*.

[8] F. B. Sperling, "The Surveyor shock absorber," in *Proceedings of the 3rd Aerospace Mechanisms Symposium*.

[9] R. B. Roncoli, "Lunar constants and models document, JPL D-32296," *Jet Propulsion Laboratory, Pasadena*, pp. 3–8.

[10] R. E. Lavender, "Monte carlo approach to touchdown dynamics for soft lunar landing," National Aeronautics And Space Administration Huntsville Al George C . . ., Tech. Rep.